Electrochemical and Mechanical Behavior in Mechanically Robust Solid Polymer Electrolytes for Use in Multifunctional Structural Batteries

James F. Snyder,* Robert H. Carter, and Eric D. Wetzel

Materials Division, U.S. Army Research Laboratory, Aberdeen Proving Ground, Maryland 21005

Received January 23, 2007. Revised Manuscript Received April 4, 2007

Polymer electrolytes were investigated for potential use in multifunctional structural batteries requiring both mechanical and electrochemical properties. Electrolytes were formulated with a broad range of multifunctional behaviors, spanning continuously from highly conductive and structurally weak materials to poorly conductive and highly structural materials. Solvent-free polymer scaffolds were synthesized from monomers containing poly(ethylene glycol) (PEG) oligomers and one to four vinyl ester groups. The electrolytes were formed by dissolving lithium trifluoromethanesulfonate in the monomers prior to thermal cure. Electrochemical, mechanical, and viscoelastic properties were studied with respect to salt concentration, polymer chemistry, and polymer architecture. The addition of salt was found to have minimal impact on compressive stiffness, whereas it increased T_g and significantly influenced ion conductivity, with a maximum conductivity at 9−12% salt w/w PEG. At a constant salt concentration, the homopolymer electrolytes exhibited close to a 1:1 inverse correlation between conductivity and stiffness as monomer composition was changed.

Introduction

Multifunctional composites are materials that inherently possess two or more distinct, beneficial functionalities.[1−4] One example is a structural battery that can both store electrochemical energy and carry mechanical loads.[1] This structural battery could potentially replace static load-bearing components in a traditional structure, such as an unmanned aerial vehicle (UAV), in order to reduce overall system weight or volume.

To create a structural battery, load-bearing properties must be engineered into the battery packaging, electrolyte, and/or electrodes. Previous examples of structural batteries have primarily relied on structural packaging.[2−4] This approach is most effective for very thin or low-mass batteries, where packaging constitutes a significant fraction of battery weight. However, for more massive batteries, significant system-level benefits are only possible through designing structural properties directly into the electrolyte and electrode materials.

The typical motivation for engineering mechanical properties into polymer electrolytes is to improve their robustness as a separator layer between electrodes.[5] Achieving high electrolyte modulus is often limited by the competing need for efficient ion transport. In solvent-free systems, polymer mobility is typically required to aid ion transport,[6] but directly leads to compromised mechanical properties. Similarly, in solvent-swollen systems, the presence of solvent results in a reduction of mechanical properties. Previous studies have utilized a range of strategies for augmenting structural properties in polymer electrolytes, including cross-linking,[7,8] ceramic particle fillers,[9,10] hybrid organic−inorganic polymers,[11,12] clay fillers,[13] fiber fillers,[14] and block copolymers.[15−18] However, these approaches have been unable to demonstrate superior mechanical properties while maintaining useful ion conductivity.

One promising class of polymers for structural electrolytes is vinyl ester derivatives of poly(ethylene glycol) (PEG). Polyacrylates have been previously studied for electrolyte use because of their dimensional stability;[19] however, they

* Corresponding author. E-mail: jsnyder@arl.army.mil.

(1) South, J. T.; Carter, R. H.; Snyder, J. F.; Hilton, C. D.; O'Brien, D. J.; Wetzel, E. D. In *2004 MRS Fall Conference*, Boston, Nov 29−Dec 3, 2004; Materials Research Society: Warrendale, PA, 2004; p 851.
(2) Qidwai, M. A.; Baucom, J. N.; Thomas, J. P.; Horner, D. M. In *Functionally Graded Materials viii*; Trans Tech Publications: Zurich-Uetikon, Switzerland, 2005; Vol. 492−493, pp 157−162.
(3) Thomas, J. P.; Qidwai, M. A. *JOM* **2005**, *57*, 18−24.
(4) Thomas, J. P.; Qidwai, M. A. *Acta Mater.* **2004**, *52*, 2155−2164.
(5) Meyer, W. H. *Adv. Mater.* **1998**, *10*, 439.
(6) Berthier, C.; Gorecki, W.; Minier, M.; Armand, M. B.; Chabagno, J. M.; Rigaud, P. *Solid State Ionics* **1983**, *11*, 91−95.
(7) Kaskhedikar, N.; Paulsdorf, J.; Burjanadze, M.; Karatas, Y.; Wilmer, D.; Roling, B.; Wiemhofer, H. D. *Solid State Ionics* **2006**, *177*, 703−707.
(8) Lenest, J. F.; Gandini, A.; Cheradame, H. *Br. Polym. J.* **1988**, *20*, 253−268.
(9) Scrosati, B.; Croce, F.; Panero, S. *J. Power Sources* **2001**, *100*, 93−100.
(10) Walls, H. J.; Riley, M. W.; Fedkiw, P. S.; Spontak, R. J.; Baker, G. L.; Khan, S. A. *Electrochim. Acta* **2003**, *48*, 2071−2077.
(11) Kennedy, C. A.; Zhan, B. Z.; White, M. A. *J. Compos. Mater.* **2005**, *39*, 193−198.
(12) Leite, E. R.; Souza, F. L.; Bueno, P. R.; de Lazaro, S.; Longo, E. *Chem. Mater.* **2005**, *17*, 4561−4563.
(13) Chaiko, D. J. *Chem. Mater.* **2003**, *15*, 1105−1110.
(14) Wen, Z. Y.; Wu, M. M.; Itoh, T.; Kubo, M.; Lin, Z. X.; Yamamoto, O. *Solid State Ionics* **2002**, *148*, 185−191.
(15) Niitani, T.; Shimada, M.; Kawamura, K.; Kanamura, K. *J. Power Sources* **2005**, *146*, 386−390.
(16) Soo, P. P.; Huang, B. Y.; Jang, Y. I.; Chiang, Y. M.; Sadoway, D. R.; Mayes, A. M. *J. Electrochem. Soc.* **1999**, *146*, 32−37.
(17) Trapa, P. E.; Won, Y. Y.; Mui, S. C.; Olivetti, E. A.; Huang, B. Y.; Sadoway, D. R.; Mayes, A. M.; Dallek, S. *J. Electrochem. Soc.* **2005**, *152*, A1−A5.
(18) Jannasch, P. *Chem. Mater.* **2002**, *14*, 2718−2724.

10.1021/cm070213o CCC: $37.00
Published on Web 06/22/2007

are typically used for reinforcement in polymer gels.[20,21] Here, a broad selection of monomers has been complexed with lithium trifluoromethanesulfonate (triflate) and thermally cured as solvent-free polymers. Long-range ion transport is enabled by the etheric oxygen groups in amorphous PEG,[6] whereas structural properties are provided by cross-linked vinyl ester networks. Varying the proportions, architecture, and functionalities of these vinyl ester/PEG constituents allows for a wide range of tailorable structural and electrolytic properties. These systems can be engineered to provide ion conductivity without the addition of secondary solvents, because the PEG etheric oxygen groups are capable of dissociating and transporting the donor salt ions.[22,23] Solvent-free preparation simplifies processing and improves the likelihood of attractive mechanical properties in the electrolyte. A solid electrolyte can be achieved through radical polymerization, or addition reaction of a second species to the vinyl group, allowing for a broad range of controllable reaction schemes and resulting material properties. The liquid resin monomer complexed with lithium salt may therefore be amenable to traditional structural composite processing approaches, such as fabric preimpregnation or vacuum-assisted resin transfer molding (VARTM).

This study examines the balance between mechanical performance and conductivity in various vinyl ester PEG derivatives complexed with lithium triflate. A lithium salt has been selected because of the high energy density and compatibility with polymer-based electrolytes achievable through lithium-based battery technologies.[24] Mechanical stiffness is used as a metric of mechanical performance, because it is easily measured using small quantities of material. State-of-the-art polymer gel electrolytes have conductivities at 10^{-3} S/cm, whereas the stiffness of structural resins reaches 4 GPa for epoxy resins and 8 GPa for thermoplastics such as PEEK. Although these values are worthwhile targets, it is not necessary to match them in order to achieve overall weight reduction within a multifunctional system, which may be accomplished though synergistic gains in conductivity, stiffness, and material dimensions. The initial room-temperature target values for this study are 1×10^{-5} S/cm and 150 MPa for a solvent-free material. The design and testing of structural electrodes, and integration of these materials into a structural composite battery, will be addressed in future publications.

Experimental Section

Materials. Table 1 lists all of the PEG vinyl ester derivatives investigated in this study. Figure 1 describes the nomenclature used and correlates the symbols with each type of monomer. The label for each structure is determined from the number of vinyl ester groups followed by a letter designation of the nature of the vinyl ester (A or M for acrylate or methacrylate, respectively; generically represented by *X*), the total number of ethylene glycol units in the monomer (generically represented by *n*), and an acronym describing additional functionality. Hydroxyl and methoxy endgroups terminating sidechains are represented by OH and OMe, respectively. Nodal groups at the intersection of cross-links are represented by BPA for bisphenol A, TMP for trimethylpropane, and PE for pentaerythritol. Pendant oligomers of PEG in comb polymers (monoacrylates, **1*X*(*n*)**) are expected to have mobility to aid in ion transport, although the macromolecules are not cross-linked for mechanical strength. Vinyl ester groups affixed to both ends of PEG (**2*X*(*n*)**) result in more mechanically robust networked scaffolds but significantly reduce the potential mobility of the polyether. Additional vinyl ester groups, affixed to the ends of PEG oligomers originating from a central point of intersection or node (**3*X*(*n*)**, **4*X*(*n*)**), lead to increased networking and potentially decreased mobility of PEG. Rigid constituents and bulky cross-links restrict overall movement and also result in a stiffer material. The length of the PEG side chain or cross-link will similarly affect PEG mobility and concentration, impacting both mechanical and electrochemical properties.

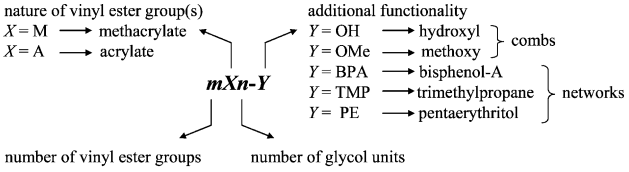

(a)

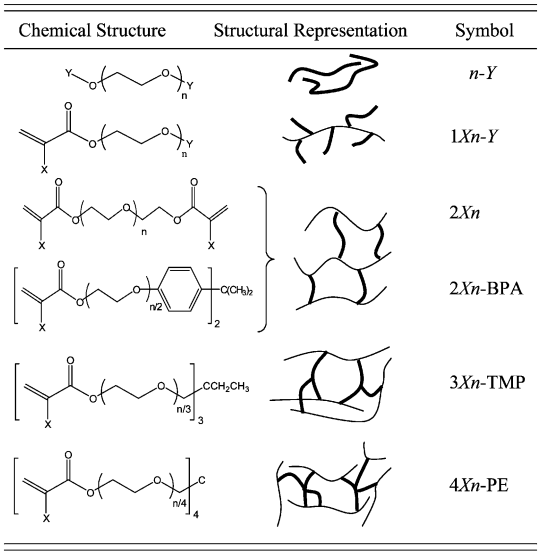

(b)

Figure 1. (a) Formulaic representation of PEG vinyl ester derivatives. (b) Chemical structures of species employed in this study and representations of their polymerized structures. Bold lines in the cartoons represent PEG regions, whereas thin lines represent polyacrylic regions. Pure PEG is included for comparison. Full conversion is assumed in the cartoons for purposes of demonstrating the impact of increasing the degree of cross-linking per molecule.

The functionalized monomers were supplied by Sartomer Company (Exton, PA), with the following product codes: monovinyl monomers CD550, CD551, CD552, CD553, CD570, CD572; divinyl monomers SR209, SR252, SR259, SR344, SR480, SR540, SR601, SR602, SR603, SR610, SR9036, CD9038; trivinyl monomers SR454, SR499, SR502, SR9035; and tetravinyl monomer SR494. According to the MSDS sheets supplied by Sartomer, the products contain 98−100% labeled component. CD570 is an

(19) Liu, G.; Reinhout, M.; Mainguy, B.; Baker, G. L. *Macromolecules* **2006**, *39*, 4726−4734.
(20) Erickson, M. J.; Frech, R.; Glatzhofer, D. T. *Polymer* **2004**, *45*, 3389−3397.
(21) Kono, M.; Hayashi, E.; Nishiura, M.; Watanabe, M. *J. Electrochem. Soc.* **2000**, *147*, 2517−2524.
(22) Fenton, D. E.; Parker, J. M.; Wright, P. V. *Polymer* **1973**, *14*, 589−589.
(23) Wright, P. V. *Br. Polym. J.* **1975**, *7*, 319.
(24) Xu, K. *Chem. Rev.* **2004**, *104*, 4303−4417.

Table 1. Properties of the Solvent-Free Vinyl Ester Polymer Electrolytes Described in Figure 1[a]

resin description	σ (S/cm) at RT	T_g (°C) w/Li	T_g (°C) w/o Li	E_{comp} (MPa) at RT	E' (MPa) 20 °C	E' (MPa) min.	E'' (MPa) peak max	tan δ peak max	M_c (g) w/o Li
Comb PEO									
monofunctional									
hydroxyl terminated sidechain									
1*X*3−OH	na/1.7×10^{-7}	na/−13	na/−18	na/45	na/17	na/2	na/420	na/1.11	na/4600
1*X*11−OH	na/7.2×10^{-6}	na/−36	na/−47	na/3.6	na/2.7	na/1.8	na/390	na/1.48	na/4200
methoxy terminated sidechain									
1*X*8−OMe	8.5×10^{-6}/4.3×10^{-6}	−46/−46	−43/−48	3.5/1.3	1.0/0.5	0.8/0.3	480/520	2.04/1.81	14 000/41 000
1*X*12.5−OMe	3.5×10^{-5}/2.3×10^{-5}	−48/−41	−50/−47	0.4/1.1	0.1/0.3	0.1/0.2	300/540	0.46/2.27	600 000/95 000
Networked PEO									
difunctional									
no node									
2*X*4.5	1.6×10^{-8}/1.3×10^{-8}	40/71	30/39	160/2100	1600/2300	42/76	190/160	0.47/0.37	200/120
2*X*9	2.6×10^{-7}/2.6×10^{-8}	−17/−3	−27/−11	30/87	14/48	14/26	320/280	0.97/0.68	350/320
2*X*13.5	1.3×10^{-6}/5.3×10^{-7}	−24/−17	−33/−24	15/25	12/11	11/9	330/340	1.27/1.04	940/640
bisphenol-A node									
2*X*4−BPA	7.0×10^{-9}/1.8×10^{-8}	26/47	24/26	690/1700	1800/2100	8/10	240/170	0.49/0.42	940/580
2*X*10−BPA	9.5×10^{-9}/1.9×10^{-8}	2/25	5/20	77/250	18/1200	7/23	270/240	1.10/0.76	550/520
2*X*30−BPA	1.7×10^{-6}/1.1×10^{-6}	−21/−18	−32/−23	15/15	9/8	7/8	370/370	1.60/1.53	1600/n/a
trifunctional									
trimethylpropane node									
3*X*3−TMP	1.6×10^{-8}/na	−4/na	−5/na	560/na	1100/na	160/na	150/na	0.21/na	64/na
3*X*6−TMP	2.9×10^{-8}/na	35/na	10/na	140/na	1400/na	43/na	150/na	0.37/na	290/na
3*X*9−TMP	3.2×10^{-8}/na	−5/na	−8/na	110/na	130/na	40/na	210/na	0.46/na	210/na
3*X*15−TMP	1.3×10^{-7}/na	−21/na	−26/na	43/na	14/na	14/na	360/na	1.13/na	290/na
tetrafunctional									
pentaerythritol node									
4*X*4−PE	5.9×10^{-9}/na	20/na	−4/na	780/na	1800/na	190/na	120/na	0.18/na	43/na

[a] Lithium triflate is at 12% w/w weight fraction PEG in each monomer unless otherwise indicated to contain no salt (w/o Li). The chart includes conductivity (σ), glass-transition temperature (T_g), compressive stiffness (E_{comp}), storage modulus (E'), loss modulus (E''), loss tangent (tan δ), and the average molecular weight between cross-links (M_c). Data for each property are listed in the style acrylate/methacrylate. "na" is substituted for data for materials in which the monomer was not available.

exception that contains 21% of a similar compound with fewer oxyethylene units. The monomers were stored between uses in a refrigerator in brown glass bottles sealed with Parafilm. Unless otherwise noted, prior to polymerization of the monomers, all chemicals were used as received and handled exclusively in a glovebox under dry nitrogen, or in an oven with a continuous nitrogen purge. After drying the polymers, care was taken to handle the materials exclusively under dry nitrogen or dry air.

In all cases, lithium triflate (Aldrich) is the lithium salt used in monomer and polymer complexes. Lithium triflate provides a favorable combination of properties including thermal and chemical stability, cost, availability, toxicity, and sensitivity toward moisture. Lithium triflate content is reported as both a simple weight fraction and as a ratio of molecules of salt to etheric oxygens (one per oxyethylene unit), Li:EO. The latter measure is more meaningful than an overall weight percent because in these materials, PEG serves the unique function of complexing salt and allowing for ion transport, and the volume fraction polyether may be as low as 30% or higher than 80%. Note that the concentration calculations are determined on the basis of idealized structures published by Sartomer Company in conjunction with densities of equivalent materials (e.g., poly(acrylic acid), pure PEG) and should be treated as approximate. These same approximated densities are also used for calculating the relative volume fractions of the various monomers in each material system.

Polymer Preparation. Lithium triflate was dried at 180 °C under vacuum for 8 h and then added to the appropriate PEG acrylate- or methacrylate-functionalized monomer in a glovebox under dry nitrogen. The components were sealed in a glass vial, mixed on a roll mixer, and gently heated (<80 °C) as necessary to fully dissolve the salt. Light exposure was minimized during this process to prevent photoinitiated polymerization, which was found to otherwise occur with some multiacrylate monomers. Time to dissolution was 24−48 h under these conditions. Thermally induced polymerization was not apparent within the initial 48 h in the absence of initiator. The solutions were degassed under vacuum at 60 °C and backfilled with nitrogen. Organic peroxide with the trade name Trigonox was added as the initiator in quantity 1.5% w/w resin, followed by 1% w/w resin dimethylaniline. The latter was added to accelerate initiation. The samples were mixed thoroughly with a spatula and poured into silicone rubber molds. The molds were relocated to an oven and heated at 80 °C for 12 h under a continuous nitrogen purge. The temperature was then raised to 110 °C for 1 h, after which the oven was allowed to cool to room temperature.

The samples were cured in the form of pellets and prismatic bars and measured precisely using a digital caliper. Pellets were ca. 12 mm in diameter and 3 mm thick, whereas the bars were ca. 60 mm long, 12 mm wide, and 4 mm thick. Samples that cured with a concave or convex surface were sanded flat. Sanding was found to have no noticeable impact on property measurement versus unsanded samples that cured with flat surfaces. Both sides of the pellets were coated with a thin application of quick drying silver paint. The pellets were heated to 90−110 °C under vacuum for at least 12 h to remove residual solvent. The superficial silver films were measured to be about 0.03 mm thick and could be peeled off easily, after which it was evident by visual inspection that silver particles did not penetrate the polymers. The silver-coated pellets were relocated to the glove box and sealed in glass vials under dry nitrogen. Each pellet was used for both impedance and compression testing, whereas the bars were used for dynamic mechanical analysis.

Material characterization was carried out in two stages. In the first stage, the effect of salt content was studied by complexing a diverse subset of monomers with lithium triflate over a concentration range of 7−35% salt w/w PEG. In the second stage, the full range of PEG vinyl ester monomers employed in this study were formulated and tested with a fixed concentration of 12% lithium triflate w/w PEG.

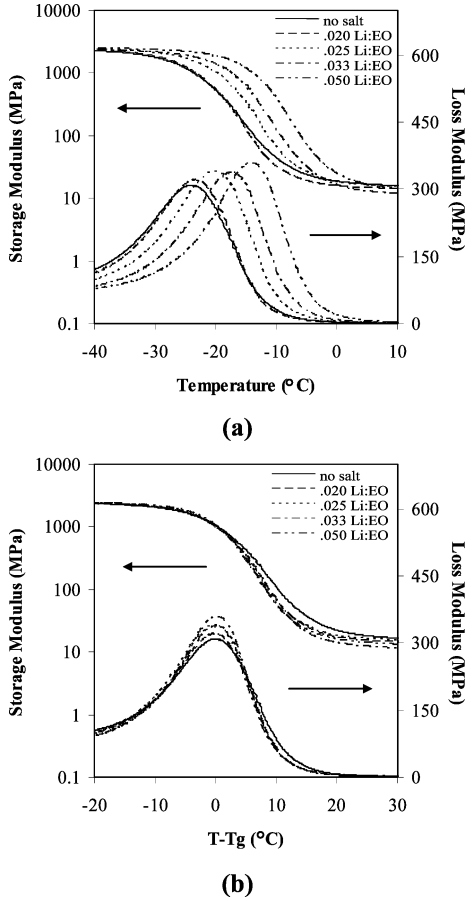

Figure 2. Storage modulus and loss-tangent variations with salt concentration for PEG 600 dimethacrylate host polymer (**2M13.5**) according to (a) temperature and (b) temperature normalized by T_g for each sample.

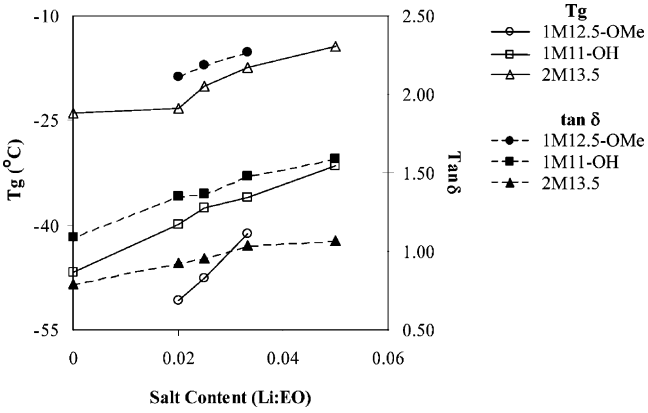

Figure 3. Impact of salt concentration on the glass-transition temperature and loss-tangent peak height for several vinyl ester polymer electrolytes described in Table 1.

Impedance Testing. Electrochemical impedance spectroscopy was conducted using a Solartron 1260 Impedance/Gain-Phase Analyzer and Solartron 1287 Electrochemical Interface across a frequency range of 1×10^6 to 10 Hz at room temperature (18−20 °C). Each sample was assembled under a dry air atmosphere (<5 ppm water) in a test cell with stainless steel blocking electrodes. Bulk resistance was extracted by fitting the impedance data to an equivalent circuit using ZPlot software. Over all of the material systems investigated, the average margin of error as calculated from the standard deviation of two or more pellets was 26%, with a median of 19%. These errors are attributed to uneven sample dimensions or cracks and defects formed during handling. However, the level of accuracy is still sufficient to make meaningful comparisons between material systems, which exhibited conductivity values over a range of 3−4 orders of magnitude.

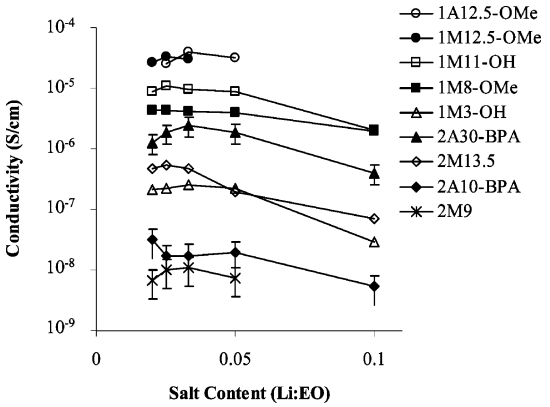

Figure 4. Impact of salt concentration on the conductivity for several vinyl ester polymer electrolytes described in Table 1. Conductivity at zero salt content was undetectable and may be considered to be 0 S/cm. Unless otherwise indicated, error bars are within the symbol size.

Compression Testing. Compression testing was conducted at room temperature using an MTS load frame with a 5 kN load cell. Each sample was exposed to the atmosphere for 2 min during compression. The tests were run in a displacement control mode at a cross-head speed of 1 mm/min. Because of the low aspect ratio of the samples, system compliance introduced error into the displacement and strain measurements. To remove this error, the instrument was evaluated each day of testing by recording displacement when no sample was placed between the crossheads. This load-displacement curve was then used to normalize the property measurements. Because of the large strains induced during the tests, the compressive stiffness for each sample was calculated from the true stress and true strain values. The average margin of error as calculated from the standard deviation of two or more pellets was 22%, with a median of 17%. The origins and impact of compression error are similar to that described above for impedance error.

Dynamic Mechanical Analysis (DMA). DMA was conducted at a single frequency across a temperature sweep using a Thermal Advantage DMA Q800 and associated software. Each rectangular sample was clamped into the sample holder and hand-tightened at room temperature. The chamber temperature was then reduced to −130 °C and the clamps were retightened to 80 psi using a torque wrench. Uncrosslinked polymers were manually retightened to a lesser pressure of approximately 20 psi to prevent cracking. The chamber temperature was then reduced to −135 °C and held at constant temperature for 1 min. Data were collected for thermal transition from −135 to 150 °C at 2 °C/min. Higher-glass-transition samples were heated to 250 °C. Samples were tested at 1 Hz using a 7.5 μm amplitude.

Fourier Transform Infrared Spectroscopy (FT-IR). Cure monitoring experiments were conducted on a Thermo Nicolet Nexus 870 equipped with an Omega CN76000 temperature controller using methods adapted from previous reports.[25,26] Samples of monomer were prepared with lithium salt and initiator immediately prior to analysis. The resulting solution was compressed between two potassium bromide transparent crystal plates. These plates were then placed in the instrument in a sample holder preheated to 80 °C. Sixteen scans were taken every 30 s in the frequency range 4000−400 cm^{-1} over the duration of the experiment. Peak heights for the carbon−carbon stretch in the vinyl groups (1637 cm^{-1}) and

(25) Brill, R. P.; Palmese, G. R. *J. Appl. Polym. Sci.* **2000**, *76*, 1572−1582.
(26) La Scala, J. J.; Sands, J. M.; Orlicki, J. A.; Robinette, E. J.; Palmese, G. R. *Polymer* **2004**, *45*, 7729−7737.

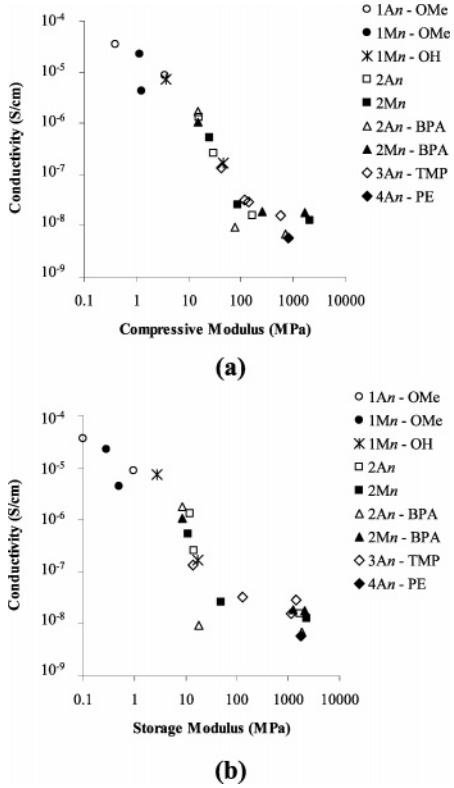

Figure 5. Conductivity vs modulus for the samples listed in Table 1 at room temperature.

out-of-plane bend in the vinyl ester groups (989 cm^{-1} for acrylates, 940 cm^{-1} for methacrylates) were monitored in real time using OMNIC 6.0 software. The temperature was maintained at 80 °C for at least an hour, at which point it was increased to 110 °C for 10 min and then to 130 °C for 10 min. It was verified that peak heights had reached a plateau before the temperature was increased.

Results

Effect of Salt Concentration. The impact of lithium triflate concentration on compression stiffness (E_c) was investigated over a range of salt concentrations corresponding to 0.020, 0.025, 0.033, 0.050, and 0.100 Li:EO for each of **1M11-OH**, **2A9**, **2M9**, **2M13.5**, **2A10-BPA**, **2A30-BPA**, and **2M30-BPA**. Values for 0.033 Li:EO are listed in Table 1. Within the limits of this study, there is no indication of meaningful or substantial change in stiffness with salt concentration.

Figure 2a presents the storage moduli (E') and loss moduli (E'') for **2M13.5** at 0.020−0.050 Li:EO and the salt-free polymer, measured using DMA. Some depression in rubbery modulus is noticeable through the addition of salt, otherwise there is minimal variation in storage modulus for either the glassy or rubbery states. This trend was also observed for most of the other polymer systems studied. The most significant effect of salt addition is a shift in the glass-transition temperature (T_g) to higher temperature values, mirrored by a similar shift in the loss tangent (tan δ) peak.[27,28] Here. we define T_g as the temperature corresponding to the peak loss modulus. Figure 2b corrects the temperature for T_g and the shift is eliminated. The peak values for loss modulus and loss tangent were also found to increase slightly with addition, with the former demonstrated by Figure 2b.

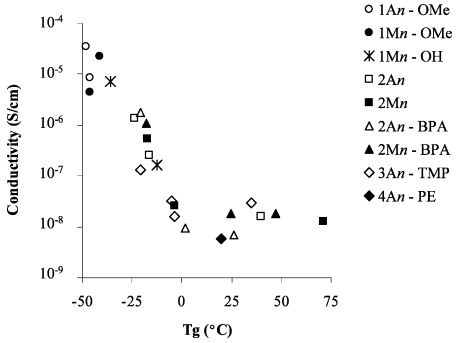

Figure 6. Conductivity vs T_g for the samples listed in Table 1 at room temperature.

Figure 3 illustrates the consistent rise in T_g with lithium concentration for **2M13.5** and two comb polymer electrolytes with similar volume fractions of PEG (78%) and polymethacrylate, **1M12.5-OMe** and **1M11-OH**. T_g and loss tangent both increase with salt concentration for all three material systems. The highest values of T_g, and lowest values of loss tangent, are noted for the most heavily cross-linked system, **2M13.5**. In contrast, the least networked system, **1M12.5-OMe**, exhibits both the lowest T_g values and highest loss tangents.

Figure 4 shows the effect of salt concentration on conductivity (σ) for both comb and networked polymer electrolytes. The room-temperature conductivity exhibits a peak value at intermediate salt levels, consistent with previous observations[29−31] and modeling results.[32] For most samples in Figure 4, the conductivity is maximized between 0.025 and 0.033 Li:EO, which is equivalent to 9−12% lithium triflate w/w PEG.

Effect of Polymer Chemistry and Architecture. Table 1 summarizes the characterization data for the full range of polymer electrolytes investigated, at a fixed salt content of 0.033 Li:EO. The table reports conductivity, compression modulus, T_g (both with and without salt), room-temperature storage modulus, peak loss tangent, and the average molecular weight between cross-links (M_c). The T_g, storage modulus, and loss tangent values are from DMA measurements. M_c is calculated according to the theory of rubber elasticity using eq 1[33,34]

$$E'_r = \frac{3RT\rho}{M_c} \quad (1)$$

in which E'_r is the modulus in the rubbery region (taken to be E'_{min}) at a given temperature (T) and polymer density (ρ),

(27) Killis, A.; Lenest, J. F.; Gandini, A.; Cheradame, H. *Makromol. Chem.−Macromol. Chem. Phys.* **1982**, *183*, 1037−1050.
(28) Masui, H.; Williams, M. E.; Long, J. W.; Troutman, M.; Murray, R. W. *Solid State Ionics* **1998**, *107*, 175−184.
(29) Snyder, J. F.; Ratner, M. A.; Shriver, D. F. *J. Electrochem. Soc.* **2003**, *150*, A1090−A1094.
(30) Cowie, J. M. G.; Spence, G. H. *Solid State Ionics* **1999**, *123*, 233−242.
(31) Angell, C. A.; Bressel, R. D. *J. Phys. Chem.* **1972**, *76*, 3244−&.
(32) Snyder, J. F.; Ratner, M. A.; Shriver, D. F. *J. Electrochem. Soc.* **2001**, *148*, A858−A863.
(33) Srobl, G. *The Physics of Polymers*, 2nd ed.; Springer: New York, 1997.
(34) Palmese, G. R.; McCullough, R. L. *J. Appl. Polym. Sci.* **1992**, *46*, 1863−1873.

Figure 5 attempts to capture the multifunctional character of the materials by plotting conductivity as a function of modulus for the full range of polymer electrolytes. Commercial materials may be considered to lie upon either the *y*-axis (liquid electrolytes) or the *x*-axis (structural resins). Figure 5a utilizes compressive stiffnesses to approximate mechanical behavior, whereas Figure 5b employs storage moduli. Logarithmic axes are used to better show the data because both properties span several orders of magnitude. Samples with better multifunctionality will tend toward the upper-right portion of the graph. The data shows simple log−log dependence of the data. A best fit line for all of the data has a slope of −1 in log−log coordinates. There is an inflection point in the data curve at a stiffness of 100 MPa, with little apparent variation in conductivity for higher stiffness polymers. Figure 6 establishes a similar trend for conductivity versus T_g, with an inflection point around 10 °C. Materials to the right of the inflection point in Figure 6 are largely in the glassy state during room-temperature measurements.

Figure 7 details the trends in compressive modulus relative to volume fractions polyether (Figure 7a), vinyl ester (Figure 7b), and both vinyl ester and bisphenol A (Figure 7c). Most samples are comprised almost entirely of these functionalities such that a reduction in volume fraction polyether relates to an increase in volume fraction vinyl ester and, when applicable, volume fraction BPA. The equivalent conductivity trends are inverted from those in Figure 7 as a result of the inverse proportionality of the electrochemical and mechanical properties. A power law regression has been included in Figure 7c to demonstrate that all of the samples follow a single trend.

Figure 8 overlays storage modulus versus reduced temperature for select polymer electrolytes. The trends were found to be consistent for all polymers studied. As the degree of branching increases for a given composition, the modulus changes over a wider temperature region and reaches a lower minimum value, as demonstrated by the four solid curves. The dashed curves have much higher vinyl ester concentrations, which result in significant broadening of the curve and some inflation of the modulus in the rubbery region.

Time-dependent analysis of conversion by FT-IR is shown in Figure 9 for several samples of varying degree of branching. The conversion, α, at time *t* was determined from the absorption peak heights, β, for a peak directly impacted by the reaction and a reference peak that is not affected by the reaction, as shown in eq 2[26]

$$\alpha = 1 - \left(\frac{\beta(t)_{\text{peak}}}{\beta(t=0)_{\text{peak}}}\right) \times \left(\frac{\beta(t=0)_{\text{reference}}}{\beta(t)_{\text{reference}}}\right) \qquad (2)$$

In Figure 9, the peak of interest is for the vinyl stretch at 1637 cm^{-1} and the reference peak is at 640 cm^{-1}. Conversion rates of the vinyl group at 30 min are 98.6, 84.1, and 88.9% for **2A4.5**, **3A3-TMP**, and **4A4-PE**, respectively. Conversion was also calculated using the bending mode for the acrylate and methacrylate groups at 989 and 940 cm^{-1}, respectively. Another peak at 940 cm^{-1} rendered the methacrylate conversions difficult to calculate accurately; however, the acrylate conversions generally supported the data respective to the vinyl stretch mode. Only samples with high vinyl ester contents are shown, because the accuracy of the experiment diminished with decreasing initial peak height of the vinyl stretching mode. Generation of reliable conversion data for

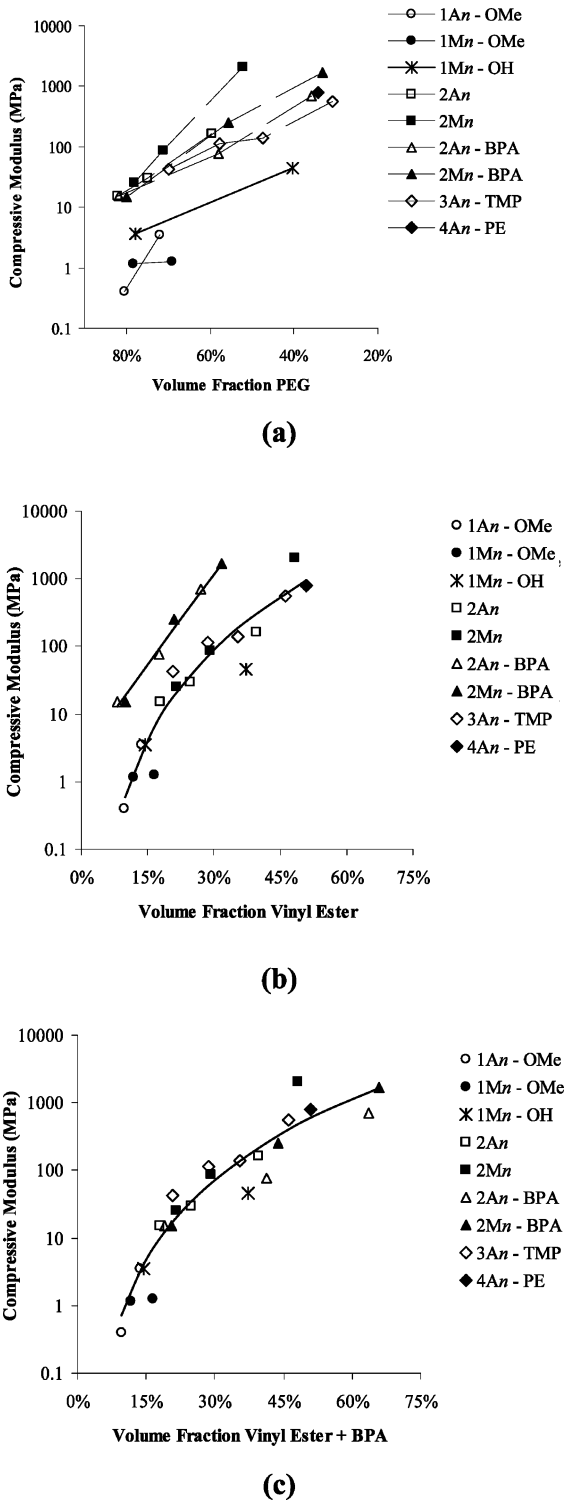

Figure 7. Modulus trends for the vinyl ester polymer electrolytes listed in Table 1, as described by volume fraction of (a) poly(ethylene glycol), (b) vinyl ester, and (c) vinyl ester and bisphenol A. The *x*-axes of (b) and (c) are reversed from that of (a) to emphasize the inverse relationship between volume fraction polyether and volume fraction vinyl ester and BPA; (b) includes a best fit exponential regression for **2*Xn*-BPA**, $y = 2.3e^{21x}$, and a best fit power law regression for all other systems, $y = 18\,000x^{4.5}$; (c) includes a best fit power law regression for all samples, $y = 9000x^{4.1}$.

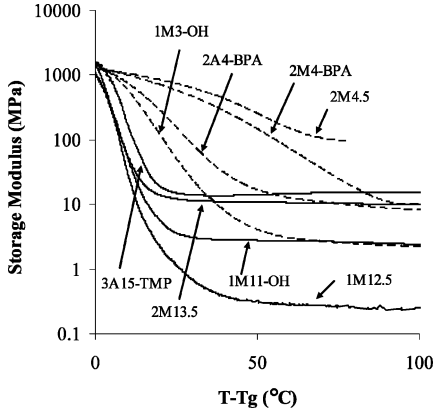

Figure 8. DMA-derived storage modulus versus reduced temperature for several vinyl ester polymer electrolytes listed in Table 1.

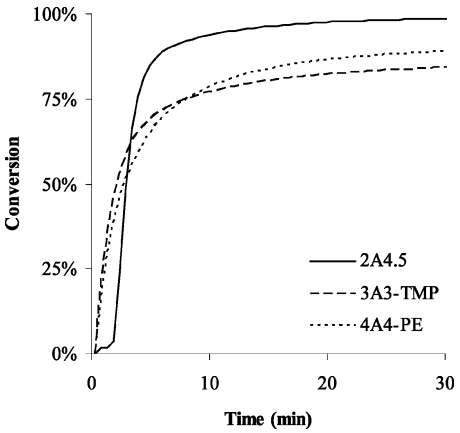

Figure 9. Vinyl ester conversion as a function of time as determined via FT-IR for several polymer electrolytes described in Table 1. The experiment was conducted at a constant temperature of 80 °C during the illustrated time period.

all samples is underway and evaluation of their relationship to material properties will be discussed within the context of a future publication.

Discussion

Effect of Salt Concentration. The results of Figures 2 and 3 show that the concentration of salt has only a minor effect on electrolyte thermomechanical properties. The increase in T_g may be attributed to ionic cross-linking by the dissolved salt particles. Ionic cross-linking is the retarding influence of cations on polymer motion when an occupied coordination site includes etheric oxygens on two or more polymer chains.[27,28] The cation occupying the site provides a temporary network between polymer chains through simultaneous ionic interaction with the oxygen groups. In spite of the increased ionic cross-link density, increasing the salt content leads to more energy damping, indicated by higher and more narrow loss modulus and loss tangent peaks. This trend is in contrast to the reduction in height of both peaks that results from covalent cross-linking, as demonstrated by the results in Table 1. The opposing effects of ionic and covalent cross-linking on energy damping are clearly evident in Figure 3 by comparing the tan δ trends within and between sample sets **1M12.5** and **2M13.5**. This contrasting behavior may derive from the proportional relationship of energy damping to polymer mobility and viscosity. Covalent cross-links reduce mobility without a corresponding impact on viscosity, thereby reducing the magnitude of damping. The effective cross-linking achieved through the introduction of salt should reduce mobility as well but the observed increase in damping suggests that there is a simultaneous and higher magnitude increase in interactions related to energy dissipation. Ionic cross-links have been previously shown to provide greater energy loss and greater stress relaxation than covalent cross-links in vulcanized carboxylated nitrile rubber elastomers.[35] We are conducting further experiments to explain the disparity in viscoelastic response with these different modes of cross-linking in the materials presented here. However, the results indicate that the addition of salt does not significantly affect mechanical stiffness for the purposes of the current study.

The results of Figure 4 show that ion conductivity is maximized at a particular salt concentration. Increasing the quantity of salt in a given polymer leads to an increase in the number of charge carriers, which results in an initial rise in conductivity values. The conductivity eventually reaches a maximum and then declines with increasing ion concentration because of the stiffening impact of ionic cross-linking and a declining number of vacant coordination sites.[32] Given that a typical coordination site in amorphous PEG is comprised of five oxyethylene units, the resins are optimized at about 15% potential capacity. The resins that reach a maximum conductivity at higher salt concentrations, such as **1A12.5-Me** and **2A30-BPA**, have oxyethylene units that are less tightly bound and in higher concentration as compared with those resins that reach a maximum conductivity at lower salt concentrations, such as **2M13.5**. Reduction in oxyethylene units may suppress formation of coordination sites by limiting the number of units available in a local region and isolate coordination sites such that conductive pathways become interrupted. Cross-linking in these systems may particularly hinder conductivity, because mobility of the polyether chains is critical to fast ion transport and the polyethers could lose considerable mobility when both ends are constrained by chemical bonds. Overall, salt concentration appears to have a more important effect on ionic conductivity than on mechanical properties. Therefore, in a multifunctional design, salt concentration should be chosen primarily on optimization of system conductivity.

The results of Table 1 show that the T_g values of some of our materials are slightly below room temperature. Because our mechanical comparison tests are conducted at room temperature, there is a possibility that subtle changes in temperature could have a profound influence on our testing results. However, careful analysis of the results shows that the percent deviation of the compressive stiffness was not noticeably higher in materials with T_g values near room temperature.

Effect of Polymer Chemistry and Architecture. The results in Figure 5 show a relatively continuous relationship between mechanical and conductive properties, with no dramatic outliers in the upper right quadrant that would represent exemplary multifunctional behavior. This con-

(35) Ibarra, L. *J. Appl. Polym. Sci.* **1999**, *73*, 927−933.

sistency is remarkable considering the diversity of variables, which include degree of branching, length and concentration of PEG, side chain endgroups, and inclusion of rigid BPA functional groups. The trends suggest that multifunctional behavior may not be improved substantially through polymer modification for neat polymer electrolytes derived from a single monomer.

The inflection points at 100 MPa in Figure 5 and 20 °C in Figure 6 probably reflect accuracy limits for impedance measurements using the apparatus employed for this study. However, the relatively flat slope for the stiffest materials, which are largely in the glassy state at room temperature, may also indicate a low-conductivity limit in these materials in which hardening may be achieved without proportional impact on ion transfer. Testing is underway to resolve this issue through more sensitive low-conductivity measurements.

The materials presented here have three components, the vinyl ester group, functional groups at cross-link nodes or terminating sidechains, and PEG. Inspection of Table 1 and Figure 7a indicates that polymethacrylates outperform polyacrylates in mechanical testing, whereas polyacrylates have better ion-transport properties. The *x*-axis discrepancy between methacrylate and acrylate counterparts in Figure 7a reflects the additional volume from the methyl group in polymethacrylates. This methyl group retards mobility of the polymethacrylate backbone and leads to stiffer materials. This stiffness is evident by increased T_g and E'_{min} in the polymethacrylates for the samples in which this comparison may be made (**1*Xn*-OMe**, **2*Xn***, and **2*Xn*-BPA**). The largest change in T_g is for the materials with the smallest polyether lengths and largest vinyl ester concentration such as **2*X*4.5** and **2*X*4-BPA**. These samples also demonstrate large relative change in compressive modulus, 12.7 and 2.4%, respectively, and lesser change in conductivity, 1.2 and 0.4%, respectively. It is apparent that for many of the resins, substituting an acrylate group for a methacrylate does not provide a 1:1 exchange in electromechanical properties. For the hardest materials, there is a clear multifunctional advantage in employing methacrylate groups, whereas for the most conductive materials, there is usually an advantage in using acrylics.

Side-chain endgroups and cross-link nodes play a significant role in polymer stiffening. The property values of the **1*Xn*-OH** polymers shown in Table 1 generally lay between the property values of the methoxy-terminated combs and the cross-linked polymers. The intermediacy of the hydroxyl-terminated combs is further illustrated in Figures 3, 7a, and 8. The increased E'_{min} and decreased E'' for the hydroxyl-terminated combs suggests some form of networking or interchain interactions, most likely hydrogen bonding through the hydroxyl endgroups. It is interesting to note that these noncovalent interactions have a different impact on viscoelastic properties than ionic cross-links and are more closely related to covalent networking. However, it is evident from Figures 5 and 7b that endgroup interactions do not significantly impact overall multifunctionality.

Figure 7b illustrates a potential advantage of using BPA cross-link nodes. The presence of BPA clearly provides significant hardening character for a given network size. Conversely, in Figure 7a the addition of BPA appears to actually reduce stiffness for a given polyether concentration. These observations are understood given that in these materials, adding a node at a static polyether concentration necessarily means a reduction in vinyl ester and less cross-linking. Accounting for the hardening character of BPA in the *x*-axis of Figure 7c collapses all 23 samples into one curve described by a very similar power law. Although BPA nodes do not affect overall multifunctional character in these samples, they may be useful as a replacement for vinyl esters when reduced cross-linking is desirable without diminishing performance. BPA may even improve multifunctional performance if used in the backbone of comb polymers, or in a different type of cross-link, such that hardening may be elevated without the corresponding reduction in side chain mobility that hinders ion transport.

Amorphous PEG is the solvent and carrier for ionic species in these materials. Accordingly, local and overall concentrations of PEG have a significant impact on the formation and continuity of ion coordination sites. The results in Table 1 confirm that for a given degree of branching (e.g., the **2*Xn*** series) incrementing the length and volume fraction of the polyether has orders of magnitude impact on conductivity. The opposite effect on modulus as illustrated by Figure 7a, as well as a reduction in T_g, reflects the compliant nature of amorphous PEG as well as the detrimental effects of increasing the polyether cross-link length. As the polyether length increases for a given polymer type (e.g., **2M*n***), the samples in this study exhibit decreasing E'_{min} and increasing M_c values. The cross-link density, ρ/M_c, is typically inversely proportional to the peak value of the loss tangent. Correspondingly, tan δ increases with decreasing cross-link density. Overall, these trends indicate that for a given degree of branching, no multifunctional impact will result through changes in PEG length as long as PEG crystallinity is suppressed.

The observed material behaviors suggest that the PEG chains remain amorphous at room temperature for most of the studied material systems. Above −50 °C, the DMA studies did not reveal signatures characteristic of a transition in PEG from amorphous to crystalline behavior, such as a secondary transition in the storage modulus or a secondary peak in the loss modulus. Furthermore, Figure 5 shows many of the materials, including all of the combs, have primary glass-transition temperatures well below room temperature. Note that room-temperature crystallinity of PEG oligomers as long as 7 oxyethylene units has been shown to be suppressed in combs with polysiloxane backbones.[36]

Although PEG appears to be in the amorphous state at room temperature in these materials, mobility of the polyacrylate and polyether chains still has a substantial impact on properties. According to the results in Table 1, incrementing the degree of networking achieves up to an order of magnitude change in conductivity and modulus, but in opposite directions. Because cross-linking takes place through the polyether, networking imposes a direct reduction in both

(36) Zhou, G. B.; Khan, I. M.; Smid, J. *Polym. Commun.* **1989**, *30*, 52−55.

polyacrylate mobility and polyether mobility. This limitation suggests that greater multifunctional performance may be achieved by designing polymer chemistries that undergo cross-linking while allowing the polyether groups to retain high mobility.

One detrimental effect of cross-linking is that it can limit overall conversion. Combs have no branch points and are expected to reach near-complete conversion without forming infinite networks, whereas cross-linked polymers form an immobilized network at partial levels of conversion.[37] Therefore, early gelation during cure can effectively eliminate the potential benefits of monomers capable of higher-order branching. This effect can be seen in the lower trend of Figure 7b, where the mechanical performance consistently tracks the volume fraction of vinyl ester independent of the degree of branching available in the monomer. Figure 9 similarly shows that for monomers of otherwise similar composition, the diacrylate demonstrates a noticeably higher conversion relative to the triacrylate and tetraacrylate. Note that unreacted vinyl ester chain ends may be adversely reactive or unstable during battery operation. Therefore, an increased risk of battery degradation could offset the mechanical benefits achieved through greater networking.

It is possible that higher conversion could be attained in networked species through more optimized cure cycles. However, it was observed during the FT-IR cure kinetics study that increasing the thermal conditions only modestly increased conversion. In addition, pellet samples resynthesized at 200 °C have demonstrated little change in the observed modulus but noticeable color change, indicating possible degradation. Evaluation of thermal stability by thermogravimetric analysis indicates that many of the materials are stable only to just above 200 °C. Ultimately, although cross-linking may be critical in the development of high modulus materials, application in electrochemical cells may require careful monomer selection and processing to yield high conversion.

Conclusion

The implementation of multifunctional, structural batteries requires the development of polymeric matrices that exhibit both ion conductivity and mechanical integrity. To create these novel structural electrolytes, a broad study was presented that seeks to simultaneously optimize both the electrochemical and mechanical properties of polymer electrolytes through the use of solvent-free vinyl ester resins. The polymer matrices under consideration contain a complex interplay of variables affecting both modulus and conductivity, including nature and concentration of the vinyl ester, length and concentration of polyether, inclusion of hardening agents, and degree of branching. Overall, it was found that increases in mechanical performance were typically accompanied by corresponding decreases in ionic conductivity. This general trend allows for the formulation of electrolytes with a broad range of multifunctional behaviors, spanning continuously from highly conductive and structurally weak materials to poorly conductive and highly structural materials.

Careful examination of the data reveals subtle trends that could prove useful for the optimization of multifunctional performance. Adding an excess of lithium salt has only a slight increase on compressive stiffness, such that conductivity may be maximized by optimizing the salt concentration without undue concern for mechanical properties. Polymethacrylates have clear multifunctional advantage over polyacrylates for harder materials, whereas high-volume fraction polyethers are better as polyacrylates. Comb polymers allow for greater polyether mobility and consequently more highly conductive materials, but with associated sacrifices in mechanical performance. Networked polymers span a wide range of properties, but increasing the degree of branching did not seem to have a significant impact on overall performance. The addition of BPA groups modified material properties in a manner similar to the addition of an equivalent volume fraction of vinyl ester. Several methods that inversely affected conductivity and thermomechanical properties are associated with chain stiffening. Including BPA functional groups, using methacrylate vinyl esters rather than acrylates, and reducing the PEG content were all found to decrease conductivity and increase thermomechanical properties. Further study of reinforcing methods may allow for longer side-chain development and more controlled architectures and properties.

The electrochemical−mechanical properties for most of the samples in this study are about an order of magnitude lower than required for multifunctional application.[38] Overall, the results suggest that a neat homopolymer electrolyte will be unlikely to fulfill the requirements of a structural electrolyte. Instead, multifunctional properties are more likely to be realized by combining monomers of different properties as copolymers. The conductivity and modulus values reported here may also be augmented through the controlled addition of liquid electrolytes and inorganic fillers, respectively. We are currently exploring these avenues.

A final consideration is the processability of these monomer systems for realistic composite fabrication operations, which typically require pressure-induced wet out of dry fabric preforms. In general, the viscosities of the unreacted systems in this study range from 10 to 1000 cP, which should be low enough to allow for traditional composite processing. Demonstration of practical composite processing using these novel multifunctional resin systems will be presented in later studies.

Acknowledgment. The authors are grateful to Dr. John La Scala, Dr. Rob Jensen, and Dr. Josh Orlicki for their advice, to Dr. La Scala for his assistance with the FT-IR cure kinetics experiments, and to Dr. Jensen for his assistance with the DMA.

CM070213O

(37) Flory, P. J. *Principles of Polymers Chemistry*; Cornell University Press: Ithaca, NY, 1953.
(38) Wetzel, E. D. *AMPTIAC Q.* **2004**, *8*, 91−95.